



Cite this: *Phys. Chem. Chem. Phys.*,  
2014, **16**, 18553

## Pressure-induced transformations in LiCl–H<sub>2</sub>O at 77 K

G. N. Ruiz,<sup>ab</sup> L. E. Bove,<sup>cd</sup> H. R. Corti<sup>ae</sup> and T. Loerting<sup>\*b</sup>

A systematic study of the properties of high-density amorphous ice (HDA) in the presence of increasing amounts of salt is missing, especially because it is challenging to avoid ice crystallization upon cooling the pressurized liquid. In order to be able to study HDA also in the presence of small amounts of salt, we have investigated the transformation behaviour of quenched aqueous LiCl solutions (mole fraction  $x < 0.25$ ) upon pressurization in a piston-cylinder setup at 77 K. The sample properties were characterized by *in situ* dilatometry under high pressure conditions and after recovery by *ex situ* powder X-ray diffraction (XRD) and differential scanning calorimetry (DSC) at ambient pressure. Two regimes can be identified, with a rather sharp switch at about  $x = 0.12$ . At  $x < 0.12$  the samples show the phenomenology also known for pure water samples. They are composed mainly of hexagonal ice ( $I_h$ ) and experience pressure-induced amorphization to HDA at  $P > 1$  GPa. The observed densification is consistent with the idea that a freeze concentrated LiCl solution of  $x = 0.14$  ( $R = 6$ ) segregates, which transforms to the glassy state upon cooling, and that the densification is only due to the  $I_h \rightarrow$  HDA transition. Also the XRD patterns and DSC scans are almost unaffected by the presence of the segregated glassy LiCl solution. Upon heating at ambient pressure HDA experiences the polyamorphic transition to low-density amorphous ice (LDA) at  $\sim 120$  K, even at  $x \sim 0.10$ . Based on the latent heat evolved in the transition we suggest that almost all water in the sample transforms to an LDA-like state, even the water in the vicinity of the ions. The glassy LiCl solution acts as a spectator that does not shift the transformation temperature significantly and experiences a glass-to-liquid transition at  $\sim 140$  K prior to the crystallization to cubic ice. By contrast, at  $x > 0.12$  the phenomenology completely changes and is now dominated by the salt. Hexagonal ice no longer forms upon quenching the LiCl solution, but instead LDA forms. A broad pressure-induced transformation at  $> 0.6$  GPa can be attributed to the densification of LDA, the glassy LiCl solution and/or glassy hydrates.

Received 25th April 2014,  
Accepted 18th July 2014

DOI: 10.1039/c4cp01786b

www.rsc.org/pccp

### 1. Introduction

Water polyamorphism is a fundamental concept when it comes to understanding supercooled water and aqueous solutions.<sup>1–4</sup> It might be responsible for several observed anomalies, whose study is relevant for astrophysics, cryobiology and many other disciplines.<sup>1–4</sup> Three amorphous ices, namely low- (LDA), high- (HDA) and very high-density amorphous ice (VHDA), have been

recognized.<sup>5</sup> One highly debated question is whether these amorphous states represent disordered forms of the corresponding crystalline phases or if they are the solid proxies of distinct liquid states in the deeply supercooled regime.<sup>1</sup> Recent dielectric and calorimetric studies at ambient pressure suggest that water indeed shows two distinct glass transitions that connect these polyamorphs with two supercooled liquids.<sup>6</sup> The study of vitrified aqueous solutions of LiCl has suggested the existence of liquid–liquid immiscibility and polyamorphism about half a century ago.<sup>7,8</sup> In particular, Angell and coworkers performed detailed studies of the behaviour of LiCl aqueous solutions, including the study of the glass transition temperature ( $T_g$ ) as a function of composition and pressure, homogeneous and heterogeneous nucleation, and ice crystallization.<sup>8–11</sup> Also Kanno inferred the existence of liquid–liquid immiscibility by studying LiCl aqueous solutions at high pressures.<sup>12</sup> These authors introduced the hydration number  $R$  (moles H<sub>2</sub>O/moles salt) as the concentration scale, which is used here, along with the linear mole fraction scale,  $x$  (moles salt/total moles). Additional work on the link between LDA–HDA polyamorphism in

<sup>a</sup> Instituto de Química Física de los Materiales, Medio Ambiente y Energía (INQUIMAE-CONICET), Facultad de Ciencias Exactas y Naturales, Universidad de Buenos Aires, Pabellón II, Ciudad Universitaria, (1428), Buenos Aires, Argentina

<sup>b</sup> Institute of Physical Chemistry, University of Innsbruck, Innrain 52a, 6020 Innsbruck, Austria. E-mail: thomas.loerting@uibk.ac.at

<sup>c</sup> Institut de Minéralogie, de Physique des Matériaux, et de Cosmochimie (IMPMC) – UMR CNRS 7590, UPMC Université P. & M. Curie, Sorbonne Universités, 4 Place Jussieu, F-75005 Paris, France

<sup>d</sup> EPFL, Institute of Condensed Matter Physics, Ecole Polytechnique Fédérale de Lausanne (EPFL), Station 3, CH-1015 Lausanne, Switzerland

<sup>e</sup> Departamento de Física de la Materia Condensada, Comisión Nacional de Energía Atómica, Avda. General Paz 1499 (1650) San Martín, Buenos Aires, Argentina

dilute LiCl-solutions and liquid–liquid immiscibility was done by Mishima in the last decade.<sup>13</sup> Bove *et al.* could also find a reversible HDA–VHDA transition in concentrated solutions ( $R = 6$ ) at 120 K and 2 GPa.<sup>14</sup>

Slow-cooling methods for preparing glassy LiCl aqueous solutions at ambient pressure faced the problem of inaccessibility of the glassy state at low salt concentrations (at the left of the eutectic point,  $R > 7$ ) due to ice crystallization and phase segregation. This problem could be avoided by using the hyperquenching method developed by Mayer in Innsbruck.<sup>17</sup> The glass transition temperatures reported by Mayer and co-workers for hyperquenched LiCl solutions with  $R > 10$ <sup>15,18</sup> complement those reported by slower cooling.<sup>7</sup>  $T_g$  shows a complex behaviour, including a minimum and a maximum, as a function of salt content in the dilute regime (see dotted line in Fig. 1).<sup>15</sup> This suggests that there is a competition between structure making and structure breaking influences of the ions on the hydrogen-bonded network.

Neutron diffraction experiments were done on concentrated solutions ( $R = 6$ )<sup>14,16</sup> and on diluted solutions ( $R = 40$ )<sup>19</sup> in the supercooled and hyperquenched states. To the right of the eutectic composition (Fig. 1,  $R < 7$ ) metastable domains and hydrates play an important role.<sup>16</sup> Conversely in the dilute regime the structure of water is slightly modified by the presence

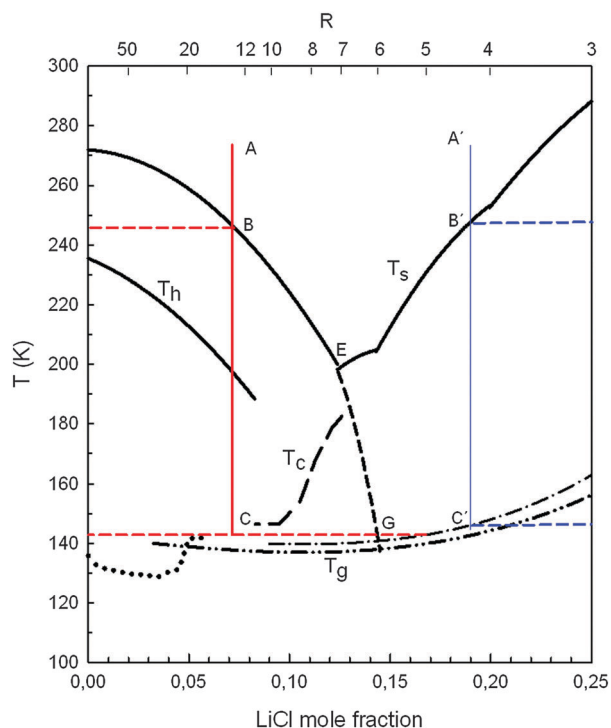


Fig. 1 Phase diagram of the LiCl–H<sub>2</sub>O system.  $T_m$ : melting line;  $T_s$ : solubility curves of the different hydrates (LiCl·xH<sub>2</sub>O);  $T_g$ : glass transition temperature (dotted line from ref. 15; dash-dot line from ref. 7; dash-dot-dot line from ref. 16).  $T_c$ : ice crystallization line from ref. 16;  $T_h$ , homogeneous nucleation line from ref. 23. E indicates the eutectic point of the mixture, the dashed line is an assumed extrapolation of the ice melting curve in the supercooled region, and G represent the maximally freeze-concentrated phase, located close to  $R = 6$ .<sup>16</sup>

of salt, and the hyperquenched sample is similar to pure LDA ice.<sup>19</sup> It is worth noting that ionic solutes affect the structure of water in a manner similar to the application of pressures<sup>20</sup> as recently confirmed by neutron diffraction measurements<sup>14</sup> and Raman measurements<sup>21</sup> on LiCl concentrated solutions.

In addition to hyperquenching aqueous solutions at ambient pressure, glasses can also be prepared by pressure amorphization. Mishima and co-workers showed that hexagonal ice can be converted to HDA at  $P > 1.2$  GPa by pressure-induced amorphization at 77 K.<sup>3</sup> A systematic study about pressure-induced amorphization at 77 K for LiCl solutions is missing and, thus, it is the main focus of the present work. Most experiments with LiCl-solutions under high-pressure conditions were performed by Suzuki and Mishima, who prepared the amorphous LiCl systems by cooling the pressurized liquid solution,<sup>13,22–25</sup> rather than by pressure-induced amorphization of the solid at 77 K. However for these high-pressure vitrification experiments, crystallization of the solution is an issue, in particular for dilute samples. This can be overcome if the amorphous LiCl–H<sub>2</sub>O samples are prepared by pressure-induced amorphization. From a study of emulsified LiCl aqueous solutions under high-pressure conditions Mishima conjectured that HDA is the state of solvent water in the high concentration electrolyte solution.<sup>26</sup> That is, the water in aqueous solutions (solvent water) is structurally related to high density liquid water, HDL, rather than to low density liquid water, LDL. This hypothesis was confirmed by the direct comparison of the measured static structure factors in concentrated solutions and in pure HDA water.<sup>14</sup> Further support comes from the analysis of the OH stretching vibrational modes of vitrified LiCl solutions ( $R \geq 10$ ),<sup>21,22</sup> DSC analysis,<sup>27</sup> and molecular dynamics studies of other aqueous electrolytes.<sup>28,29</sup>

Nanophase segregation in supercooled LiCl aqueous solutions has been studied recently using large-scale molecular dynamics simulations,<sup>30</sup> and transient grating experiments.<sup>31</sup> These studies started to give some insights into the relationship between the formation of nanosegregated glasses and the polyamorphism of water.

Thermodynamic and kinetic anomalies were also addressed in this supercooled system, such as its glass forming ability, fragility (viscosity vs. temperature behavior)<sup>32,33</sup> and dynamic crossover.<sup>34</sup>

While LiCl solutions have been studied systematically at low pressure, the behaviour of dilute solutions is less clear under the influence of pressure. We, therefore, investigated phase transitions of quenched aqueous LiCl solutions after pressurization at 77 K. For that purpose we have employed the protocol, which results in pressure-induced amorphization at 77 K (according to the method by Mishima *et al.*<sup>35</sup>) for LiCl mole fraction in the range between 0.00 and 0.25 ( $R > 3$ ).

## II. Experimental section

We use a piston cylinder apparatus in conjunction with a high-pressure dilatometer to study the phase transformations of the quenched LiCl solutions. Initially, 500  $\mu$ l of aqueous solution

(or pure water) are pipetted into an indium container, which is kept at 77 K. The procedure is similar to the one originally developed by Mishima *et al.*<sup>35</sup> The cooling rate in this process can be estimated to be of the order of 10–100 K s<sup>-1</sup>, *i.e.*, the solutions are quenched relatively slowly. The indium container and the rather incompact solid sample are then pushed into the bore of the steel-cylinder of 8 mm in diameter. By applying about 0.3 GPa at 77 K the solid sample is compacted to a cylinder with practically no pores, dissolved air or cracks. The indium serves the purpose of largely eliminating friction between the sample and steel-cylinder walls and, thus, to avoid unwanted shock-waves propagating through the sample upon compression. The basic idea of this procedure is to apply pressures of up to 1.6 GPa at 77 K to produce amorphous material. For this purpose we used a universal material testing machine (Zwick, model BZ100/TL3S) which applies a vertical force at a controlled rate. Phase transitions upon pressurization or depressurization are monitored *in situ* by observing the relative piston displacement, *i.e.*, by using the testing machine as a dilatometer. The testing machine records the force (max. 100 kN) and the position of the piston with a reproducibility of  $\pm 0.5 \mu\text{m}$  and a spatial resolution of  $0.01 \mu\text{m}$ . This method produces unrelaxed HDA in the case of pure water samples. Klotz *et al.*<sup>36</sup> have shown quench-recovery of amorphous ice results in a kinetically arrested state when done at temperatures not higher than 100 K. For this reason samples are finally recovered from the pressure vessel and transported to a Dewar where they are kept at liquid nitrogen temperature. The absence of any phase transitions upon decompression at 77 K is confirmed here by the absence of steplike changes in the piston-displacement in the decompression.

After the pressurization–depressurization cycle the amorphous samples were studied as recovered state *ex situ* under ambient pressure conditions by X-ray diffraction using a commercial powder X-ray diffractometer Siemens, model D5000, equipped with a low-temperature Anton Paar chamber. The sample holder made of nickel plated copper was cooled to  $\sim 80$  K with liquid nitrogen. The diffractometer has an incident wavelength of  $\lambda = 1.54178 \text{ \AA}$  (CuK $\alpha$ ). During the measurement the X-ray source and the detector were set up in  $\theta/\theta$  arrangement and a Goebel mirror ensures no distortion of the Bragg reflections due to non-parallel beams.

As a second *ex situ* method the amorphous samples were studied using differential scanning calorimetry (DSC) in a Perkin-Elmer model DSC-4. For that purpose the samples were transferred under liquid nitrogen from the storage Dewar into open aluminum crucibles. These crucibles were then cold-loaded to the DSC at  $< 90$  K and scanned from 93 to 253 K at  $30 \text{ K min}^{-1}$  to investigate phase transitions at ambient pressure. In the case of pure water samples this procedure shows three exotherms corresponding to the polyamorphic transition from HDA to LDA, the crystallization of LDA to cubic ice, and the transformation from cubic ice to hexagonal ice. After recooling the sample to 93 K at  $100 \text{ K min}^{-1}$ , a second scan was performed up to 313 K. The second heating trace serves as a baseline for the first heating trace in the range 93–253 K

because no transformations can be observed in this scan. In the temperature range 253–313 K the melting endotherm of the solid solution is observed, which is used to calculate the mass of the solid solution and to normalize the DSC traces. To that end, the latent heat of melting for pure water was taken as  $5877 \text{ J mol}^{-1}$  and calculated from the data given by Monnin *et al.* for aqueous LiCl solutions.<sup>37</sup>

### III. Results

#### A. Compression experiments

Solutions with salt concentrations up to  $x = 0.25$  were prepared at ambient pressure and temperature. These solutions were used as starting materials for compression experiments. Fig. 2 shows a set of compression curves for different concentrations of LiCl. The decompression curve for  $x = 0.250$  is also shown. The black dotted line at the bottom corresponds to the compression curve of a blind experiment, *i.e.* compression of the

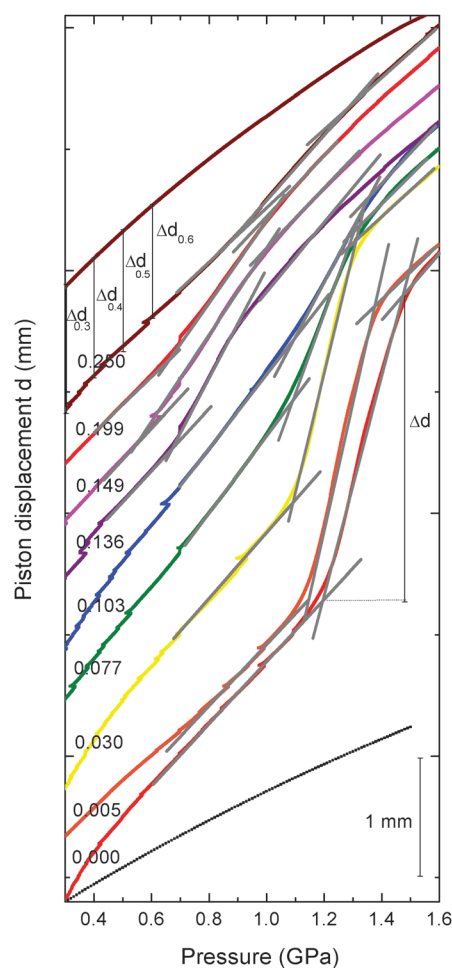


Fig. 2 Compression curves for different concentrations expressed as the LiCl mole fraction. The small kinks in the curves are associated with audible clicking noises and related to build-up and release of tension due to friction. Only for  $x = 0.250$  the decompression curve is also shown. All curves are shifted for clarity. Dotted black line: blind experiment (taken from ref. 38).

metal parts of the cell and piston, the indium container, but no ice sample.<sup>38</sup>

The change in slope for pure water starting around 1.2 GPa is in agreement with literature and portrays the amorphization transition experienced by the ice  $I_h$  sample as it densifies to HDA.<sup>35</sup> The way the slope of the amorphization curve flattens with increasing LiCl concentration is evident to the naked eye. At the same time, the onset pressure for the pressure induced amorphization shifts to lower values with increasing concentration. Three tangents were drawn on top of the compression–decompression curves, so as to be able to determine the onset and the end point of the transition. We define the *Piston displacement*  $\Delta d$  as the change in the piston position between the onset and end point positions. That is,  $\Delta d$  represents the densification of the sample experienced at the phase transition in the upstroke. Equivalently, all  $\Delta d_p$  represent the difference between the piston position in the up- and downstroke run at a specific pressure (as indicated in Fig. 2).

The values obtained for onset/end point pressures for all compression–decompression curves at all studied concentrations are shown in Fig. 3, where two different regimes can be clearly distinguished.

The first one, which we call the *water-dominated regime*, includes the concentration range  $x < 0.12$ . Within this regime the onset and endpoint pressures drop continuously by about 10% for very dilute solutions (up to a mole fraction of 0.01) and then remain relatively constant in the range  $0.01 < x < 0.12$ . The second one, the *salt-dominated regime*, covers the range  $0.12 < x < 0.25$ . Within this regime the onset and endpoint pressures drop suddenly by about 40% at  $x = 0.13$ , then slightly increase between  $x = 0.13$  and  $x = 0.25$ . These two regimes roughly correspond to what was called non-glass forming and glass-forming regimes by Angell and Sare.<sup>8</sup> At  $x < 0.12$  crystalline material experiences pressure-induced amorphization, similar to the case of pure water, whereas at  $x > 0.12$  the phase transition is experienced by the glassy material.

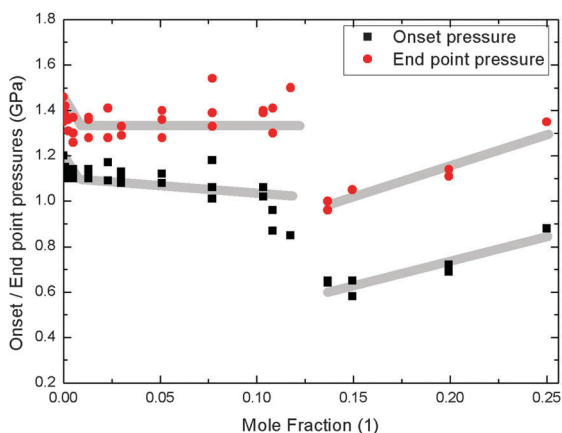


Fig. 3 Onset and end point pressures for transformations of LiCl–H<sub>2</sub>O samples upon pressurization at 77 K. Values are extracted from the intersections of the tangents in Fig. 2. The broad lines are guides to the eye. Single points represent independent measurements.

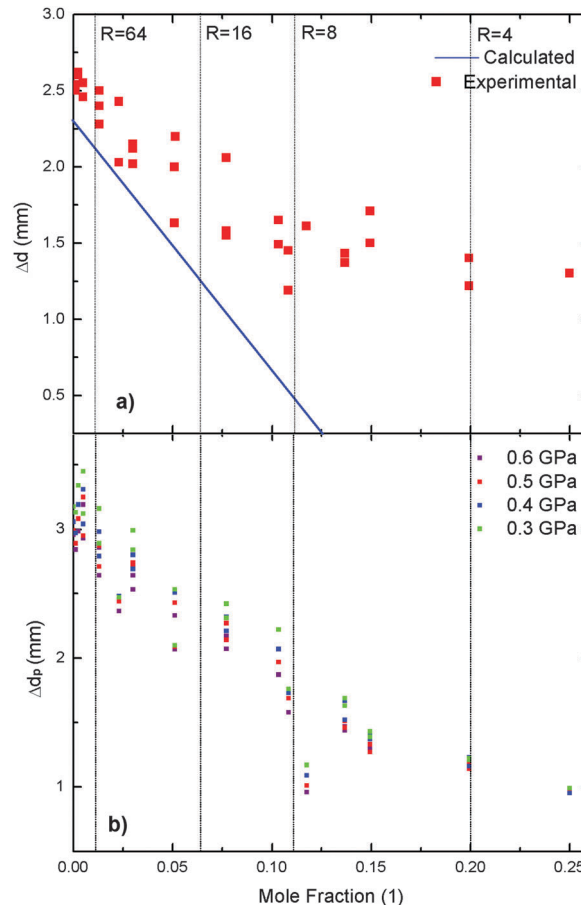


Fig. 4 (a) Piston displacement as a function of the salt concentration. The blue line shows calculated values (see text). (b) Values of  $\Delta d_p$  (see Fig. 2) at different pressures as a function of the salt concentration. Single points represent independent measurements.

The measured  $\Delta d$  for all compression–decompression curves, the calculated values for this parameter, and  $\Delta d_p$  at 0.6, 0.5, 0.4, and 0.3 GPa for all studied concentrations are shown on Fig. 4a and b respectively.

The calculated values of  $\Delta d$  were obtained assuming that the piston displacement at a given pressure corresponds to the difference in the molar volume (density) or piston displacement between ice  $I_h$  and HDA. The molar volume change at the transition ( $\sim 1.2$  GPa) is determined to be  $4.20 \text{ cm}^3 \text{ mol}^{-1}$  from Fig. 2 (a pure water curve minus the blind experiment). For comparison the molar volume difference between  $I_h$  and HDA at ambient pressure is  $3.84 \text{ cm}^3 \text{ mol}^{-1}$ .<sup>39</sup> The amount of ice  $I_h$  that separates from the solution at concentration  $R$  was calculated by assuming that upon cooling ice separates and the remaining solution reaches a final concentration of  $R_f = 6$  (see Fig. 1). The number of moles of water,  $n_w$ , that separate from the solution is given by:

$$n_w = (R - R_f)n_s \quad (1)$$

where  $n_s$  is the number of moles of LiCl in the initial (and final) solution. A constant volume of LiCl solution was employed in the experiments and the corresponding masses of the components of the mixtures were obtained from densities reported by

Conde.<sup>40</sup> Volume changes in the LiCl concentrated component were ignored. Finally, the mean piston displacement at amorphization is calculated with the following expression:

$$\Delta d = \frac{n_w \Delta V}{A} \quad (2)$$

where  $\Delta V$  is taken to be  $4.20 \text{ cm}^3 \text{ mol}^{-1}$ , and  $A$  is the area of the piston.

The good match between calculated and experimental values indicates that the assumption of glassy LiCl-patches of  $R \sim 6$  present in the sample,<sup>16,41–45</sup> which underlies the calculation, is reasonable for  $x < 0.12$ . At  $x > 0.12$  the slope of the calculated values no longer matches the data, indicating the change of regime.

Fig. 4b shows the difference in piston displacement between the upstroke and the downstroke curves at specific pressures. By contrast to the sudden change in the piston position (shown in Fig. 4a) these values indicate the permanent (non-elastic) densification of the sample. It is evident that the permanent densification decreases with increase in salt concentration. It is also evident that the permanent densification levels off at the highest salt concentrations studied here. Even at  $x = 0.25$  a permanent densification remains, that amounts to about 8% overall sample densification (which compares to 25% permanent densification in the pure water case).

## B. Ex situ X-ray characterization

X-Ray diffractograms were recorded for samples of different concentrations before and after pressurization. All measurements were done at 77 K and 0.1 MPa. Fig. 5 shows the diffractograms of five samples in the salt- and water-dominated regimes before and after pressurization.

Star symbols (\*) correspond to sharp Bragg reflections of hexagonal ice at  $2\theta = 22.8^\circ$ ,  $24.3^\circ$ ,  $25.9^\circ$  and  $33.5^\circ$ . This is caused by water condensation on top of the sample when transferring it to the chamber. The (o) symbol for the sharp Bragg reflection at  $2\theta = 31.9^\circ$  stands for indium that may have been transferred from the capsule into the sample holder.

Fig. 5a–c in red present diffraction patterns very closely related to that of pure hexagonal ice. The weak intensity of the reflection at  $24.3^\circ$  is due to texture. In Fig. 5c an amorphous background is present in all angles ranging from  $20$  to  $35^\circ$ , which indicates that a very small fraction of the sample transforms to glassy LiCl even in the dilute regime.

Clearly, there is a change in the nature of the starting material depending on LiCl concentration. While solutions in the water-dominated regime generate a dominantly crystalline structure when cooled at 77 K and 0.1 MPa, the ones on the salt-dominated regime produce amorphous samples. This is consistent with the results of slow-cooling experiments reported in the literature.<sup>7,8,16</sup> A scheme of the starting material at characteristic  $R$  values is shown in Fig. 6, top row. In the case of pure water at  $R = \infty$  pure hexagonal ice forms. Introduction of some solute results in small patches of glassy LiCl (as is evident in Fig. 5c) within the matrix of hexagonal ice. In the salt-dominated regime no crystalline ice is formed. The pure water component, which is now the minor

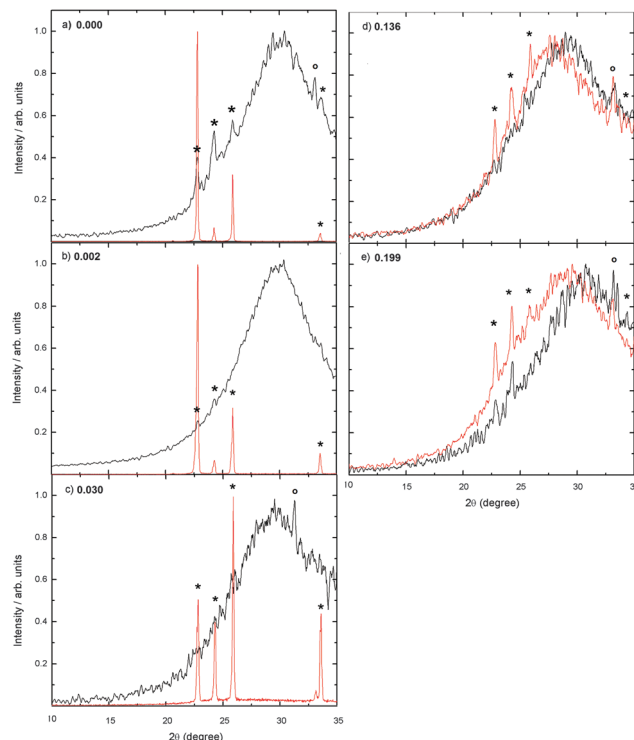


Fig. 5 X-Ray diffraction patterns of samples with LiCl mole fractions of 0.000, 0.002, 0.030, 0.136 and 0.199. All graphs in red correspond to XRDs prior to compression, while the ones in black are after pressurization. Sharp Bragg reflections marked by black stars (\*) at  $2\theta = 22.8^\circ$ ,  $24.3^\circ$ ,  $25.9^\circ$  and  $33.5^\circ$  portray the presence of hexagonal ice and o at  $31.9^\circ$  stands for indium contamination.

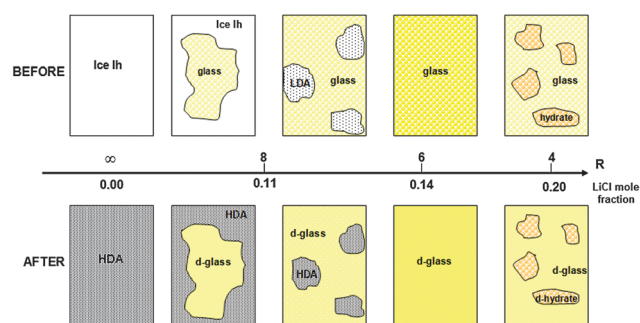


Fig. 6 Scheme of the LiCl–H<sub>2</sub>O system before and after pressurization at 77 K at some representative salt concentrations in the water- and salt-dominated regimes.

component, vitrifies to form LDA, whereas the matrix is composed of glassy LiCl, which might be described as ions solvated by HDA.<sup>25</sup> Formation of LDA is expected since pure water also transforms to LDA if it is cooled fast enough to avoid crystallization.<sup>17</sup> The necessary cooling rates for vitrification are  $10^7 \text{ K s}^{-1}$  for pure water, but much less in the presence of salt. In the salt-dominated regime the rate of  $10\text{--}100 \text{ K s}^{-1}$  employed here is sufficient for vitrification. The formation of nano-segregated LDA-domains and ion-rich vitrified solution is also confirmed from simulations of mW water in the presence of a strongly hydrophilic solute that mimics LiCl ions.<sup>46</sup> For concentrations higher than the eutectic

point also the patches of LDA disappear, and progressively more and more patches of LiCl hydrates segregate within the glassy LiCl matrix. In the vicinity of the eutectic point LiCl·5H<sub>2</sub>O segregates, whereas near  $x \sim 0.25$  LiCl·3H<sub>2</sub>O forms preferentially.<sup>47</sup>

The phase-changes seen in Fig. 2 upon pressurization, and evident in Fig. 5 from the “before” and “after” X-ray diffractograms, lead to the structures schematized at the bottom of Fig. 6. A pure water sample frozen to ice I<sub>h</sub> transforms to homogeneous HDA after pressure induced amorphization. As salt concentration increases less and less ice I<sub>h</sub> is formed, and hence  $\Delta d$  in Fig. 4 decreases linearly with salt content. The phase transformation can be associated with the ice I<sub>h</sub> phase, whereas the segregated LiCl component ( $R = 6$  according to Fig. 1) does not densify substantially. The powder X-ray patterns for the  $R = 6$  solution and for pure HDA are very similar, and also their densities are very similar. For LiCl concentrations between  $x = 0.11$  and  $x = 0.14$  ( $R = 6$  and  $R = 8$ ) ice no longer segregates from the solution upon cooling at ambient pressure. Instead a concentrated LiCl glass and LDA patches form. Upon pressurization the LDA patches are transformed into HDA, and the LiCl patches densify slightly. Between  $x \sim 0.14$  and  $x \sim 0.25$  the solution directly forms a homogeneous glass when cooled, with patches of LiCl-hydrates. The densification upon compression in Fig. 2 is very broad, which indicates that this might be related to a continuous (permanent) densification of the hydrates. These hydrates form segregated patches upon cooling inside a LiCl glass matrix. When compressed both phases densify.

Fig. 7 shows the collected powder X-ray diffractograms after pressurization, in a stacked manner, over the whole range of salt concentration. The closed squares indicate the position of the halo peaks.

The halo remains approximately constant, with a slight shift to lower angles for concentrations within the water dominated regime. On the salt dominated regime at  $x > 0.14$  the halo maximum shifts to higher angles.

The halo peak positions extracted from Fig. 7 are presented in Fig. 8 as a function of LiCl concentration. The kink in this

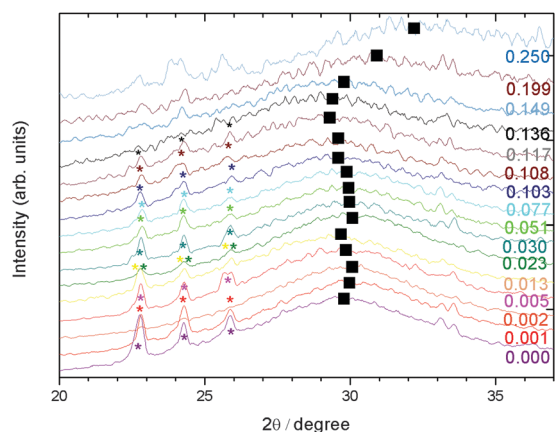


Fig. 7 XRDs indicating the shift of the corresponding halo maxima as a function of LiCl mole fraction.

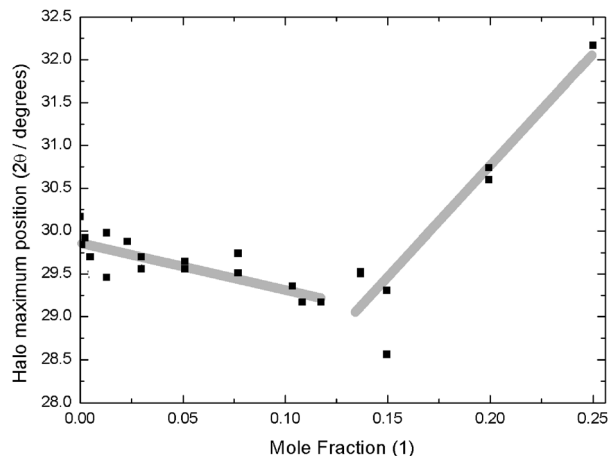


Fig. 8 Halo maximum position as a function of LiCl mole fraction. Broad lines indicate trends as guides to the eye. Single points represent individual measurements.

plot again demonstrates that the mechanism and the type of transformation are different: it changes from pressure-induced amorphization at  $x < 0.125$  to densification of amorphous material at  $x > 0.125$ . That is, the break appears near the eutectic point (see Fig. 1).

### C. Ex situ differential scanning calorimetry

Further evidence of the scheme proposed in Fig. 6 can be found by analyzing Fig. 9, where DSC scans of samples from pure water to the 0.250 LiCl mole fraction are shown.

In the pure water case the initial sample is HDA. As the sample is heated an exotherm with an onset temperature of  $\sim 121$  K is observed. This release of internal energy is the

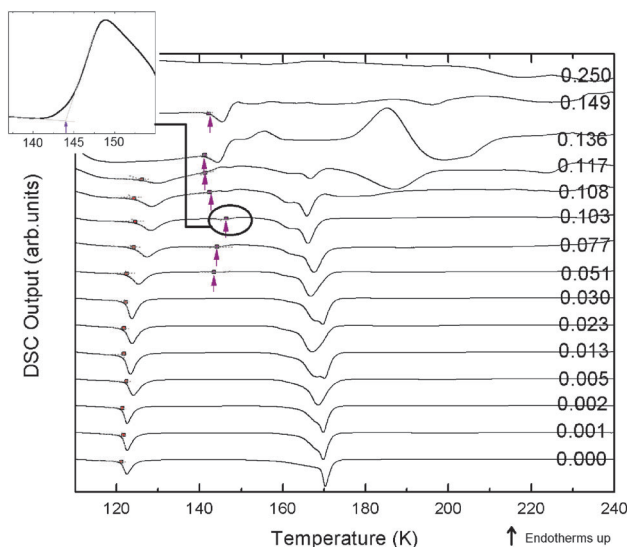


Fig. 9 DSC scans (heating rate 30 K min<sup>-1</sup>) of recovered samples after pressurization to 1.6 GPa for concentrations from  $x = 0$  to  $x = 0.25$ . Red points indicate the onset temperature for HDA → LDA transition and violet arrows indicate  $T_g$  onset temperature in samples of concentrations higher than  $x = 0.051$ .

signature of the high (HDA) to low density (LDA) transition experienced by the amorphous sample. For pure HDA we obtained  $480 \text{ J mol}^{-1}$  as the heat of transformation. This is in good agreement with the value of  $530 \pm 20 \text{ J mol}^{-1}$  reported by Handa *et al.*<sup>48</sup> The heat then significantly increases with increasing LiCl concentration up to  $2000 \text{ J mol}^{-1}$  at  $x = 0.10$  (see Table 1). Please note that latent heats are defined here per mol of water that segregates from the solution  $n_w$  (see eqn (1)). Only  $n_w$  moles of water freeze upon cooling, and only  $n_w$  moles of water experience a melting transition at  $T_m$  (see Fig. 1). The remainder of the water becomes hydration water in LiCl-6H<sub>2</sub>O patches and instead experiences a liquid-glass transition upon cooling below 140 K and a glass-liquid transition upon heating above 140 K. Our observation that the HDA → LDA latent heat per mole of freezable water ( $n_w$ ) increases so much with  $x$  indicates that not only the freezable water experiences the polyamorphic transition, but also some of the glassy hydration water. When assuming segregation of LiCl-6H<sub>2</sub>O (*i.e.*,  $R_f = 6$ ) the latent heats can be converted to a per mole of water (freezable plus unfreezable) basis by multiplication with  $(1 - R_f/R)$ . These values are given in brackets in Table 1. In the molar fraction range from 0–0.11 the latent heats for the HDA → LDA conversion remain practically constant, which implies that not only the HDA patches, but also the hydration water of the LiCl experiences the HDA → LDA transition. The nature of the transition is not entirely clear from DSC measurements alone. However, the fact that it is observed at the temperature of the HDA-LDA transition and that the latent heat is similar to the latent heat of the HDA-LDA transition suggests that also the hydration water experiences a transition from a denser, HDA-like, state to a less dense, LDA-like, state. Above 140 K this glassy hydration water then experiences the glass-liquid transition. Upon further heating another exotherm with a minimum temperature of  $\sim 170 \text{ K}$  appears, indicating crystallization of the amorphous ice into cubic ice, I<sub>c</sub>. In the pure water case the latent heat of  $1216 \text{ J mol}^{-1}$  obtained here (see Table 1) is again similar to the value of  $1370 \pm 60 \text{ J mol}^{-1}$  measured in earlier

studies for the crystallization of LDA.<sup>48,49</sup> Again, the presence of the salt increases this heat on a per mole of freezable water basis, but not as much as for the HDA → LDA transformation. This suggests that some part of the hydration water around the ions crystallizes, but not all. On a per mole of total water basis the latent heat associated with crystallization starts to decrease significantly for  $x > 0.03$ . This implies that a significant fraction of the hydration water around the ions does not crystallize. This difference with increasing  $x$  (compare columns LH<sub>1</sub> and LH<sub>2</sub> in Table 1) is due to the glass-to-liquid transition of the glassy LiCl-H<sub>2</sub>O patches at  $\sim 140 \text{ K}$  (see violet arrows in Fig. 9 and the inset to Fig. 9). Some water molecules within these patches have enough mobility above the glass transition temperature to crystallize and contribute to LH<sub>2</sub>. This is also evident as an increasing secondary peak at a minimum temperature of  $\sim 160 \text{ K}$  (see Fig. 9). The exotherm portraying the phase transformation from I<sub>c</sub> into I<sub>h</sub> is very feeble compared to HDA → LDA and LDA → I<sub>c</sub> and cannot be seen on the level of magnification shown in Fig. 9. In magnified thermograms (not shown) a tiny exotherm pertaining to the cubic ice to hexagonal ice transition is seen. That is, cubic ice crystallizes also in the presence of LiCl from the amorphous matrix. The temperature of the transformation from cubic to hexagonal ice depends strongly on the LiCl concentration. When adding the salt to the solutions the qualitative picture remains the same. The transformation from HDA to LDA can be clearly identified up to  $x \sim 0.11$ , and disappears above 0.12 (consistently with what was proposed in Fig. 6). The HDA → LDA transformation slightly shifts from 121 K in pure water to 124 K at  $x = 0.12$  (see Table 1) and broadens from 4 K to 15 K. For  $x < 0.10$  there are relatively large patches of pure HDA within the sample along with glassy LiCl patches, where the hydration water resembles HDA. That is, there is no homogenization induced by the movement of the piston densifying the sample in the course of pressure-induced transformation, but rather the segregation persists even after compression to 1.6 GPa at 77 K. Clearly, diffusive motion of ions does not take place, and also no scrambling is induced by the 25% increase in the density of the ice matrix upon amorphization. For  $x > 0.12$  the dominating structure is a homogeneous LiCl glass or a LiCl glass with LiCl hydrated patches, and hence the DSCs do not resemble any more those of an HDA sample. Instead, the glass-to-liquid transition of the LiCl glass upon heating can be seen with an onset of about 140 K for the two traces at  $x \sim 0.13$  and 0.14. This corresponds to the transition also noticed by Mishima.<sup>50</sup> Very weak signatures of this glass transition can also be seen for the DSC traces between  $x \sim 0.05$  and 0.11, thereby, demonstrating the presence of the glassy LiCl patches also at lower concentrations. Since they are hard to see on the level of magnification the glass-transition onset is marked by arrows in Fig. 9. This indicates that with increasing molar fraction more and more water is trapped within the glassy LiCl-H<sub>2</sub>O patches and that a decreasing fraction of water experiences the HDA → LDA transformation. This is again consistent with the sketch shown in Fig. 6. The crystallization of this solution is seen as a broad exotherm at  $\sim 180 \text{ K}$ . This exotherm is absent for the

**Table 1** Onset temperature ( $T_1$ ), width ( $\Delta T_1$ ), latent heat (LH<sub>1</sub>) for the HDA → LDA transition and latent heat (LH<sub>2</sub>) for the LDA → I<sub>c</sub> transition. Latent heats are given per mol of freezable water. Values in brackets are given per mole of water and calculated by multiplication with  $(1 - 6/R)$ , which assumes segregation of LiCl-6H<sub>2</sub>O. The amount of freezable water is determined from the ice melting endotherm. Uncertainties are  $\pm 0.5 \text{ K}$  for onset temperatures and  $\pm 100 \text{ J mol}^{-1}$  for latent heats

$x$	$T_1$ (K)	$\Delta T_1$ (K)	LH <sub>1</sub> (kJ mol <sup>-1</sup> )	LH <sub>2</sub> (kJ mol <sup>-1</sup> )
0.000	120.9	3.7	0.480 (0.480)	1.216 (1.216)
0.001	121.2	3.5	0.630 (0.626)	1.383 (1.374)
0.002	121.2	3.5	0.615 (0.605)	1.385 (1.364)
0.005	121.9	4.2	0.663 (0.643)	1.452 (1.408)
0.013	121.4	4.4	0.735 (0.676)	1.521 (1.400)
0.023	121.5	4.9	0.821 (0.705)	1.637 (1.405)
0.030	121.9	4.3	0.884 (0.719)	1.640 (1.335)
0.051	122.1	6.6	1.161 (0.786)	1.860 (1.260)
0.077	123.2	8.2	1.965 (0.981)	2.246 (1.121)
0.103	123.3	9.6	1.969 (0.606)	2.144 (0.660)
0.108	123.4	12.3	2.266 (0.614)	2.179 (0.591)
0.117	123.9	15.1	4.321 (0.885)	2.290 (0.469)

traces with  $x < 0.11$ . This again implies that not only the LDA fraction, but also to some extent the hydration layers of the salt crystallize together at  $\sim 170$  K. At  $R = 3$  ( $x = 0.25$ ) the glass-to-liquid transition is no longer evident in the DSC trace, because the system is now composed of glassy LiCl-hydrates. That is, also the DSC traces show a major break at  $x \sim 0.11$ , where the phenomenology at  $x < 0.11$  is water-like and the influence of the salt is barely visible in the thermograms.

## IV. Discussion

We have undertaken a study of pressure-induced transformation of aqueous LiCl solutions at 77 K. The main motivation for doing this is the accessibility of very dilute high-pressure solid solutions of amorphous LiCl–H<sub>2</sub>O. These are not accessible from other routes such as vitrification of pressurized LiCl solutions, which typically crystallize at  $x > 0.08$ .<sup>3</sup> As indicated by Fig. 5 in the solutions with LiCl concentrations lower than  $x \sim 0.11$  the material that is formed when pipetting the solution into the indium capsule at 77 K and 0.1 MPa is mainly hexagonal ice, with a small fraction of amorphous LiCl/H<sub>2</sub>O patches. The salt does not affect substantially the phenomenology: pressure-induced amorphization at 77 K takes place as in the pure water case. The amorphization onset shifts to slightly lower pressures with the addition of salt (see Fig. 2 and 3); DSC scans resemble those obtained for pure HDA, with only some small shifts (see Fig. 9). We call this regime the “water-dominated regime”. By contrast, very suddenly at  $x \sim 0.12$  ( $R \sim 8$ ) the salt starts to dominate the phenomenology; the breakpoint is about the same as the point found by Angell and Sare which delineates glass-forming from non-glass forming regime for solutions vitrified at ambient pressure.<sup>8</sup> We call this the “salt-dominated regime”. Instead of a sharp pressure-induced amorphization process, we observe a broad densification of the sample upon compression (Fig. 2). This densification of HDA on the salt-dominated regime is in agreement with earlier publications.<sup>14,26,51</sup> The nature of the initial sample (prior to pressurization at 77 K) can be explained by resorting to the LiCl phase diagram in Fig. 1. It can be observed that for concentrations lower than the eutectic ( $x_E \sim 0.125$ ), like sample A, cooling through the red line A–C should lead to separation of ice I<sub>h</sub> and a LiCl solution whose concentration would gradually increase with the amount of hexagonal ice separated. If temperature drops to values lower than the eutectic temperature ( $T_E \sim 197$  K) the solution would keep on concentrating (dashed line), eventually reaching  $T_g$ . The point where the extrapolated melting curve crosses the glass transition curve corresponds to the maximum freezing concentration. In the case of initial solutions with LiCl concentration higher than the eutectic (like sample A'), LiCl hydrates separate upon cooling following the blue line A'–C'. As opposed to what would happen on the water-dominated regime, the separation of LiCl hydrates would render the remaining solution more diluted as compared to its original concentration.

Bearing in mind the phase diagram of the LiCl–H<sub>2</sub>O system presented in Fig. 1 and relating it to what is observed in Fig. 3,

one can have a more clear idea of the mechanisms causing this break on the two regimes. In Fig. 3 it may be observed that the end point pressure for concentrations higher than  $x = 0.12$  follows an increasing trend. If the salt- and water-dominated regimes are divided by the eutectic concentration, further addition of salt causes the formation of hydrates. We emphasize that, depending on cooling rates, sample volumes and sample purity, ice may crystallize anywhere between the melting line  $T_m$  and the homogeneous nucleation line  $T_h$  (see Fig. 1). It is unclear where the homogeneous nucleation line  $T_h$  intersects the glass transition line  $T_g$  in LiCl/H<sub>2</sub>O.<sup>23</sup> Using our experimental parameters we find complete vitrification at  $x > 0.12$  (see Fig. 7) and segregation of (some) hexagonal ice up to  $x \sim 0.12$  (see Fig. 3).

The homogeneity/heterogeneity of the sample after pressure induced amorphization is a matter that needs to be considered. One could imagine that the movement of the piston and the densification of the sample by up to 25% could result in a scrambling and possibly homogenize the sample. Whether this is indeed the case is hard to tell from X-ray patterns since amorphous LiCl/6H<sub>2</sub>O and HDA show very similar patterns. However, the DSC scans (Fig. 9) indicate the simultaneous presence of LiCl–H<sub>2</sub>O patches and LDA at 130 K. The latent heat LH<sub>1</sub> associated with the HDA → LDA transition on a per mole of water basis does not change with increasing molar fraction, which implies that also the hydration water in the vicinity of the ions experiences the polyamorphic transition. This finding is unexpected because earlier work had shown that the hydration water is HDA-like even under ambient pressure conditions.<sup>34,50</sup> By contrast, only part of the hydration water crystallizes together with LDA to cubic ice, and so the latent heat LH<sub>2</sub> associated with crystallization decreases with increasing molar fraction. In the sketch shown in Fig. 6 we consider the sample to be inhomogeneous after pressurization, *i.e.*, consisting of pure HDA-patches and LiCl/6H<sub>2</sub>O patches. Alternatively, the LiCl could be dissolved homogeneously in a HDA matrix, as also conjectured by Mishima. If macroscopic patches of amorphous ice and macroscopic patches of LiCl solution were present, then Porod scattering at low diffraction angles ( $2\theta < 15^\circ$ ) should be visible in the XRD patterns of the amorphous samples. Porod scattering is absent in our measurements in the range 10–15° (see Fig. 5), which might be a hint at homogeneous nature. However, Porod scattering might still appear at  $2\theta < 10^\circ$ , and so we cannot infer a homogeneous nature of the HDA/LiCl sample. Bove *et al.* have shown phase separation between clusters with a low solute concentration and a remaining, more concentrated, solution for mole fractions lower than 0.140.<sup>31</sup> In the water-dominated regime at  $x < 0.12$  the phenomenology is almost unaffected by the presence of the salt. Patches of glassy LiCl merely act as a spectator. The onset and endpoint for amorphization of the ice patches remain practically constant, with the exception of a 10% downshift at  $x < 0.01$ . Also the powder patterns for the amorphous material after pressurization are practically identical. Furthermore, DSC scans look remarkably similar, no matter whether a pure water sample or a sample containing up to a 0.12 mole fraction of LiCl is studied. The phase behaviour is the same for all samples in the water-dominated

regime, except that a weak glass transition appears at  $\sim 140$  K that pertains to the glassy LiCl patches. The onset temperature for transformation of the salty HDA to salty LDA increases by just 2 K between the pure water case and  $x = 0.11$ , and also the crystallization temperature of LDA is not affected much. That is, the technique of judging about pure water properties from data on aqueous LiCl is highly suitable, provided the mole fraction of LiCl is small enough to remain in the water-dominated regime, which is barely affected by the presence of segregated patches of glassy LiCl solution.

## Acknowledgements

We are grateful to C. Austen Angell for valuable discussions. We want to thank the ERC Starting Grant SULIWA, FWF Start award (Y391) and the joint ANR/FWF project (I1392), ANR Blanc International PACS and ANPCyT (PICT 1291) for the funding provided. HRC is a member of CONICET. This work has been supported by the ANR Contract No. ANR-13-IS04-0006-01.

## References

- 1 P. G. Debenedetti, Supercooled and glassy water, *J. Phys.: Condens. Matter*, 2003, **15**, R1669.
- 2 T. Loerting and N. Giovambattista, Amorphous ices: experiments, numerical simulations, *J. Phys.: Condens. Matter*, 2006, **18**, R919.
- 3 O. Mishima, Polyamorphism in water, *Proc. Jpn. Acad., Ser. B*, 2010, **86**, 165.
- 4 P. Ball, *H<sub>2</sub>O: a biography of water*, Phoenix, London, Fifth edn, 2004.
- 5 T. Loerting, K. Winkel, M. Seidl, M. Bauer, C. Mitterdorfer, P. Handle, C. Salzmann, E. Mayer, J. L. Finney and D. T. Bowron, How many amorphous ices are there?, *Phys. Chem. Chem. Phys.*, 2011, **13**, 8783.
- 6 K. Amann-Winkel, C. Gainaru, H. Nelson, P. Handle, M. Seidl, R. Böhmer and T. Loerting, Water's second glass transition, *Proc. Natl. Acad. Sci. U. S. A.*, 2013, **110**, 17720.
- 7 C. A. Angell and E. J. Sare, Liquid-liquid immiscibility in common aqueous solutions at low temperatures, *J. Chem. Phys.*, 1968, **49**, 4713.
- 8 C. A. Angell and E. J. Sare, Glass Forming Composition Regions and Glass Transition Temperatures for Aqueous Electrolyte Solutions, *J. Chem. Phys.*, 1970, **52**, 1058.
- 9 H. Kanno and C. A. Angell, Homogeneous nucleation and glass formation in aqueous alkaline halide solutions at high pressure, *J. Phys. Chem.*, 1977, **81**, 2639.
- 10 J. Dupuy, J. F. Jal, C. Ferradou, P. Chieux, A. F. Wright, R. Calemczuk and C. A. Angell, Controlled nucleation and quasi-ordered growth of ice crystals from low temperature electrolyte solutions, *Nature*, 1982, **296**, 138.
- 11 D. R. MacFarlane, R. K. Kadiyala and C. A. Angell, Direct observation of time-temperature-transformation curves for crystallization of ice from solutions by a homogeneous mechanism, *J. Phys. Chem.*, 1983, **87**, 1094.
- 12 H. Kanno, Double glass transitions in aqueous lithium chloride solutions vitrified at high pressures: evidence for a liquid-liquid immiscibility, *J. Phys. Chem.*, 1987, **91**, 1967.
- 13 O. Mishima, Phase separation in dilute LiCl-H<sub>2</sub>O solution related to the polyamorphism of liquid water, *J. Chem. Phys.*, 2007, **126**, 244507.
- 14 L. E. Bove, S. Klotz, J. Philippe and A. M. Saitta, Pressure-Induced Polyamorphism in Salty Water, *Phys. Rev. Lett.*, 2011, **106**, 125701.
- 15 K. Hofer, A. Hallbrucker, E. Mayer and G. P. Johari, Vitrified dilute aqueous solutions. 3. Plasticization of water's hydrogen-bonded network and the glass transition temperature's minimum, *J. Phys. Chem.*, 1989, **93**, 4674.
- 16 B. Prevel, J. F. Jal, J. Dupuy-Philon and A. K. Soper, Structural characterization of an electrolytic aqueous solution, LiCl-6H<sub>2</sub>O in the glass, supercooled liquid, and liquid states, *J. Chem. Phys.*, 1995, **103**, 1886.
- 17 E. Mayer, New method for vitrifying water and other liquids by rapid cooling of their aerosols, *J. Appl. Phys.*, 1985, **58**, 663.
- 18 K. Hofer, G. Astl, E. Mayer and G. P. Johari, Vitrified dilute aqueous solutions. 4. Effects of electrolytes and polyhydric alcohols on the glass transition features of hyperquenched aqueous solutions, *J. Phys. Chem.*, 1991, **95**, 10777.
- 19 K. Winkel, M. Seidl, T. Loerting, L. E. Bove, S. Imberti, V. Molinero, F. Bruni, R. Mancinelli and M. A. Ricci, Structural study of low concentration LiCl aqueous solutions in the liquid, supercooled, and hyperquenched glassy states, *J. Chem. Phys.*, 2011, **134**, 024515.
- 20 R. Leberman and A. K. Soper, Effect of high salt concentrations on water structure, *Nature*, 1995, **378**, 364.
- 21 Y. Suzuki and Y. Tominaga, Polarized Raman spectroscopy study on the solvent state of glassy LiCl aqueous solutions and the state of relaxed high-density amorphous ices, *J. Chem. Phys.*, 2011, **134**, 244511.
- 22 Y. Suzuki and O. Mishima, Raman spectroscopy study of glassy water in dilute lithium chloride aqueous solution vitrified under pressure, *J. Chem. Phys.*, 2002, **117**, 1673.
- 23 O. Mishima, Application of polyamorphism in water to spontaneous crystallization of emulsified LiCl-H<sub>2</sub>O solution, *J. Chem. Phys.*, 2005, **123**, 154506.
- 24 O. Mishima, Differences between pressure-induced densification of LiCl-H<sub>2</sub>O glass and the polyamorphic transition of H<sub>2</sub>O, *J. Phys.: Condens. Matter*, 2011, **21**, 155105.
- 25 O. Mishima, Melting of the precipitated ice IV in LiCl aqueous solution and polyamorphism of water, *J. Phys. Chem. B*, 2011, **115**, 14064.
- 26 O. Mishima, The glass - to - liquid transition of the emulsified high - density amorphous ice made by pressure - induced amorphization, *J. Chem. Phys.*, 2004, **121**, 3161.
- 27 H. R. Corti, F. Nores Pondal and C. A. Angell, Heat capacity and glass transition in P<sub>2</sub>O<sub>5</sub>-H<sub>2</sub>O solutions: support for Mishima's conjecture on solvent water at low temperature, *Phys. Chem. Chem. Phys.*, 2011, **13**, 19741.
- 28 D. Corradini, M. Rovere and P. Gallo, Structural Properties of High and Low Density Water in a Supercooled Aqueous Solution of Salt, *J. Phys. Chem. B*, 2011, **115**, 1461.

- 29 P. Longinotti, M. A. Carignano, I. Szleifer and H. R. Corti, Anomalies in supercooled NaCl aqueous solutions: a microscopic perspective, *J. Chem. Phys.*, 2011, **134**, 244510.
- 30 L. Le and V. Molinero, Nanophase segregation in supercooled aqueous solutions and their glasses driven by the polyamorphism of water, *J. Phys. Chem. A*, 2011, **115**, 5900.
- 31 L. E. Bove, C. Dreyfus, R. Torre and R. M. Pick, Observation of nanophase segregation in LiCl aqueous solutions from transient grating experiments, *J. Chem. Phys.*, 2013, **139**, 044501.
- 32 M. Kobayashi and H. Tanaka, Possible link of the V-shaped phase diagram to the glass-forming ability and fragility in a water-salt mixture, *Phys. Rev. Lett.*, 2011, **106**, 125703.
- 33 M. Kobayashi and H. Tanaka, Relationship between the phase diagram, the glass-forming ability, and the fragility of a water/salt mixture, *J. Phys. Chem. B*, 2011, **115**, 14077.
- 34 E. Mamontov, Diffusion dynamics of water molecules in a LiCl solution: A low-temperature crossover, *J. Phys. Chem. B*, 2009, **113**, 14073.
- 35 O. Mishima, L. D. Calvert and E. Whalley, Melting ice I at 77 K and 10 kbar: a new method of making amorphous solids, *Nature*, 1984, **310**, 393.
- 36 S. Klotz, T. Straessle, A. M. Saitta, G. Rousse, G. Hamel, R. J. Nelmes, J. S. Loveday and M. Guthrie, *In situ* neutron diffraction studies of high density amorphous ice under pressure, *J. Phys.: Condens. Matter*, 2005, **17**, S967.
- 37 C. Monnin, M. Dubois, N. Papaiconomou and J. P. Simonin, Thermodynamics of the LiCl + H<sub>2</sub>O system, *J. Chem. Eng. Data*, 2005, **47**, 1331.
- 38 K. Winkel, W. Schustereder, I. Kohl, C. G. Salzmann, E. Mayer and T. Loerting, *Isothermal amorphous - amorphous - amorphous transitions in water*, *Physics and Chemistry of Ice*, The Royal Society of Chemistry, Cambridge, 2007, p 641.
- 39 T. Loerting, M. Bauer, I. Kohl, K. Watschinger, K. Winkel and E. Mayer, Cryoflotation: densities of amorphous and crystalline ices, *J. Phys. Chem. B*, 2011, **115**(48), 14167.
- 40 M. R. Conde, Properties of aqueous solutions of lithium and calcium chlorides: formulations for use in air conditioning equipment design, *Int. J. Therm. Sci.*, 2004, **43**, 367.
- 41 A. Elarby-Aouizerat, J. F. Jal, P. Chieux, J. M. Letoffé, P. Claudy and J. Dupuy, Metastable crystallization products and metastable phase diagram of the glassy and supercooled aqueous ionic solutions of LiCl, *J. Non-Cryst. Solids*, 1988, **104**, 203.
- 42 B. Prevel, J. Dupuy-Phillon, J. F. Jal, J. F. Legrand and P. Chieux, Structural relaxation in supercooled glass-forming solutions: a neutron spin-echo study of LiCl, 6 D<sub>2</sub>O, *J. Phys.: Condens. Matter*, 1994, **6**, 1279.
- 43 A. Honnersteid, J. Nuss, C. Muhle and M. Jansen, Die Kristallstrukturen der Monohydrate von Lithiumchlorid und Lithiumbromid, *Z. Anorg. Allg. Chem.*, 2003, **629**, 312.
- 44 J. F. Jal, A. K. Soper, P. Carmona and L. Dupuy, Microscopic structure of LiCl-6D<sub>2</sub>O in glassy and liquid phases, *J. Phys.: Condens. Matter*, 1991, **3**, 551.
- 45 B. Prevel, J. F. Jal, P. Carmona, J. Dupuy-Philon and A. K. Soper, Medium and long range correlations in the electrolyte LiCl-4H<sub>2</sub>O: Transition to the glass regime, *J. Chem. Phys.*, 1995, **103**, 1897.
- 46 G. Bullock and V. Molinero, Low-density liquid water is the mother of ice: on the relation between mesostructure, thermodynamics and ice crystallization in solutions, *Faraday Discuss.*, 2013, **167**, 371.
- 47 H. E. Moran Jr, System Lithium Chloride - Water, *J. Phys. Chem.*, 1956, **60**(12), 1666.
- 48 Y. P. Handa, O. Mishima and E. Whalley, High-density amorphous ice III. Thermal properties, *J. Chem. Phys.*, 1986, **84**, 2766.
- 49 C. G. Salzmann, I. Kohl, T. Loerting, E. Mayer and A. Hallbrucker, The low-temperature dynamics of recovered ice XII as studied by differential scanning calorimetry: a comparison with ice V, *Phys. Chem. Chem. Phys.*, 2003, **5**, 3507.
- 50 Y. Suzuki and O. Mishima, Sudden switchover between the polyamorphic phase separation and the glass - to - liquid transition in glassy LiCl aqueous solutions, *J. Chem. Phys.*, 2013, **138**, 084507.
- 51 Y. Yoshimura and H. Kanno, Pressure-induced amorphization of ice in aqueous LiCl solution, *J. Phys.: Condens. Matter*, 2002, **14**, 10671.